

Supplementary materials

Fig. S1. MEI4 foci quantification

(A) MEI4 foci per nucleus were counted in wild type, *Sycp3*^{-/-}, *Smc1β*^{-/-}, *Dmc1*^{-/-}, *Syce2*^{-/-}, *Mei1*^{-/-} and *Mei4*^{-/-} leptotene spermatocytes (p values are from two-sided Mann-Whitney tests; n: number of nuclei).

(B) MEI4 axis-associated foci per nucleus were counted in wild type, *Sycp3*^{-/-}, *Smc1β*^{-/-}, *Dmc1*^{-/-}, *Syce2*^{-/-}, *Rec8*^{-/-} and *Mei1*^{-/-} leptotene spermatocytes (p values are from two-sided Mann-Whitney tests; n: number of nuclei).

Fig. S2. Formation of MEI4 foci in *Smc1β*^{-/-} and *Sycp3*^{-/-} spermatocytes

The number of MEI4 foci was reduced in leptotene spermatocytes of *Smc1β*^{-/-} mice compared to wild type animals (A) and strongly reduced in zygotene-like stage spermatocytes of *Smc1β*^{-/-} mice (B, C). (D) The intensity of MEI4 axis associated foci was measured in wild type (black) and *Smc1β*^{-/-} (grey) and the percentage of foci is plotted as a function of intensity in arbitrary units and ranked in eight bins. Intensity distributions were significantly different in wild type and *Smc1β*^{-/-} (p<0.0001, two sided Mann-Whitney test). Like in wild type animals, MEI4 and HORMAD1 were detected on nuclear spreads from *Sycp3*^{-/-} spermatocytes at leptotene (E) and at a lower level at the zygotene-like stage (F). Scale bar: 10 μm.

Fig. S3. Formation of MEI4 foci is HORMAD1-independent in preleptotene spermatocytes and MEI4 foci are displaced from axes in the absence of DMC1 or SYCE2

(A) MEI4 was detected after immunoprecipitation of protein extracts from testes of wild type, *Mei4*^{-/-} or *Hormad1*^{-/-} adult mice using a crosslinked anti-MEI4 antibody. Detection of SYCP3 was used as loading control. The increase amount of MEI4 in *Hormad1*^{-/-} testes extract relative to wild type may result from the relative higher proportion of spermatocytes in the mutant testes due to the meiotic arrest phenotype.

MEI4 localization on meiotic chromosome spreads prepared after *in vitro* EdU labeling of testis cells from wild type (B) and *Hormad1*^{-/-} mice (C). Scale bar: 10 μm

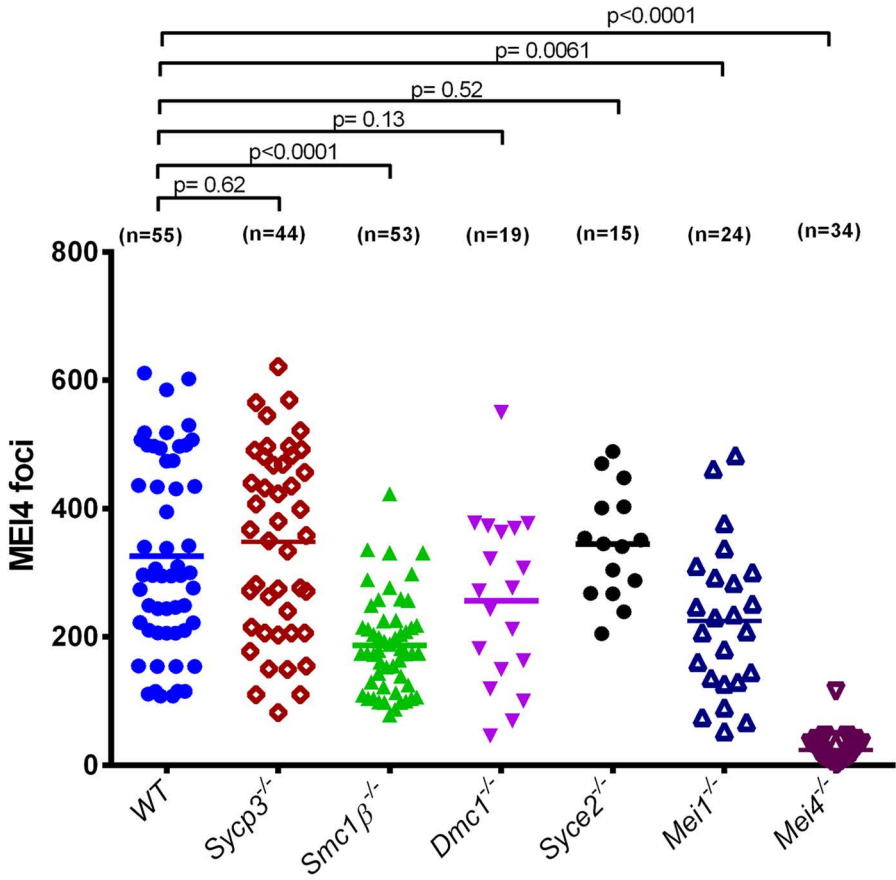
Immunostaining with anti-MEI4 and anti-SYCP3 antibodies of chromosome spreads from *Dmc1*^{-/-} (D) and *Syce2*^{-/-} (E) spermatocytes. Scale bar: 10 μm

Fig. S4. Functions of axis-associated MEI4

MEI4 foci are detected already in pre-leptotene spermatocytes and become associated with chromosome axes at leptotene. This association requires *Rad21L* and *Rec8*, *Hormad1* and *Mei1*, but not *Spo11* or *Sycp3*. Defects in MEI4 axis-association correlate with reduction of DSB activity (except for the *Spo11*^{-/-} mice). In wild type spermatocytes, MEI4 is displaced from synapsed axes at zygonema, along with HORMAD1, and might contribute to lowering DSB activity locally and as synapsis elongates. (a) from Kumar et al., 2010. (b) DSB levels are estimated based on quantification of DMC1 and RAD51 foci; (c) DSB levels are estimated from quantification of Spo11-oligo complexes; (d) DSB levels are estimated based on detection of γH2AX, RAD51 and RPA.

Fig. S1

A



B

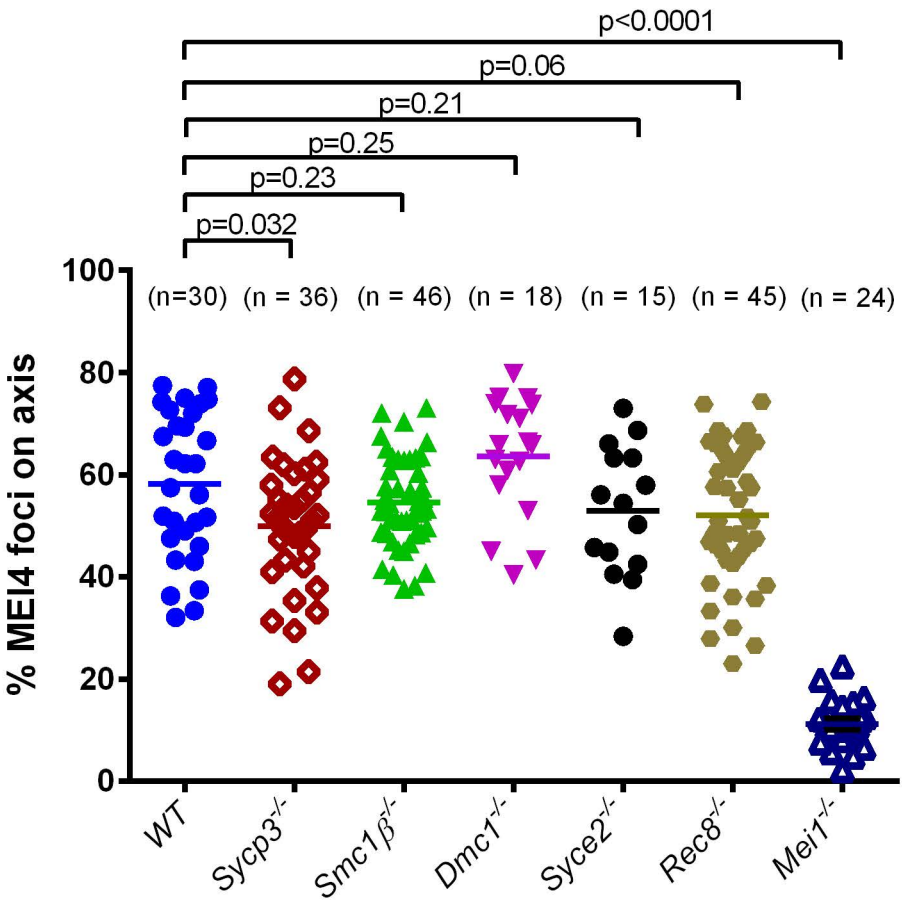


Fig. S2

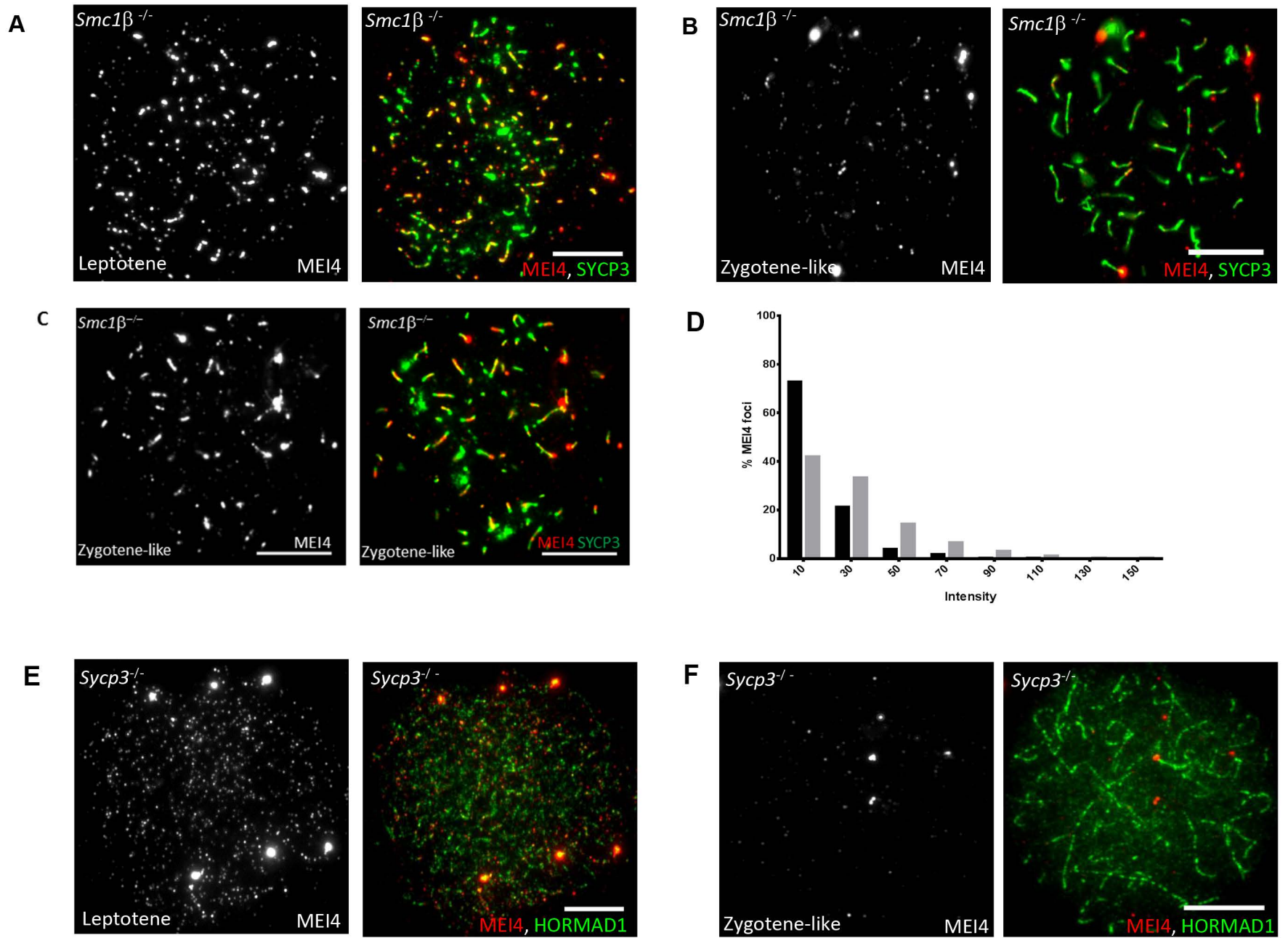
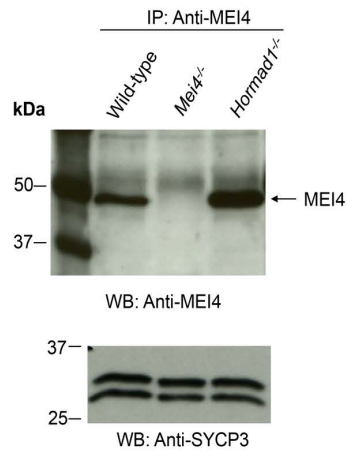
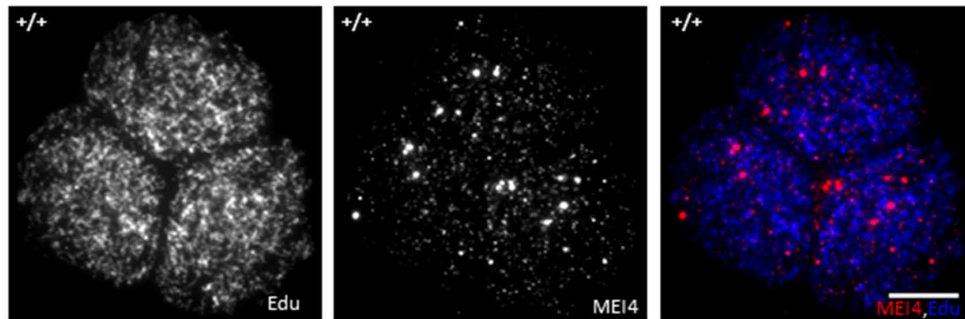


Fig. S3

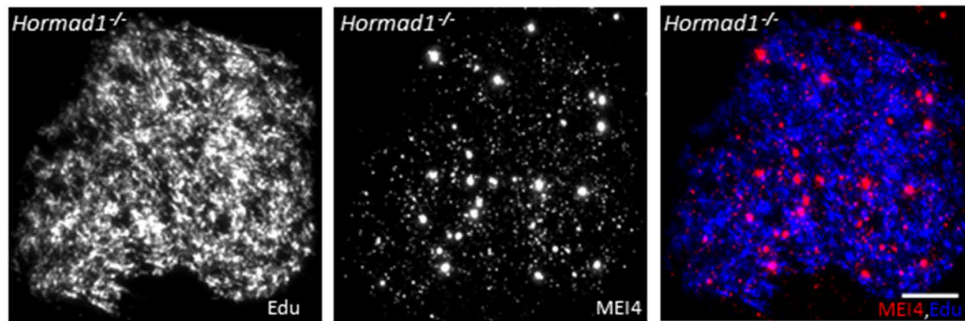
A



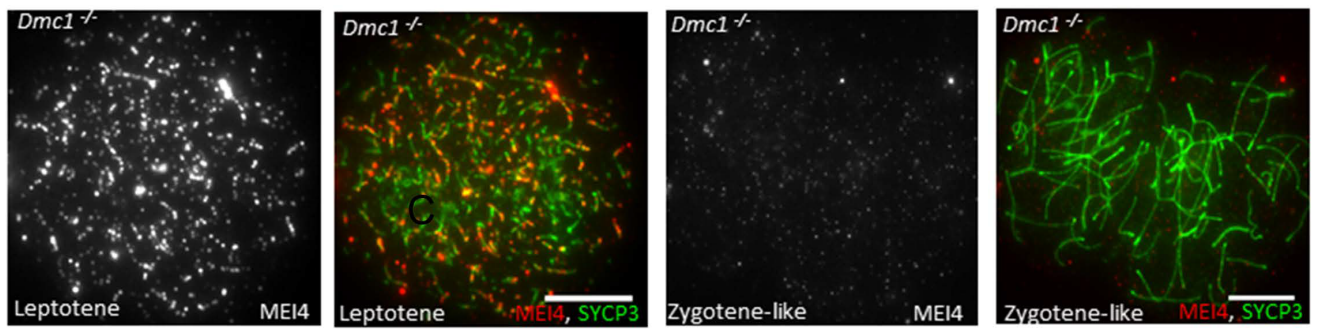
B



C



D



E

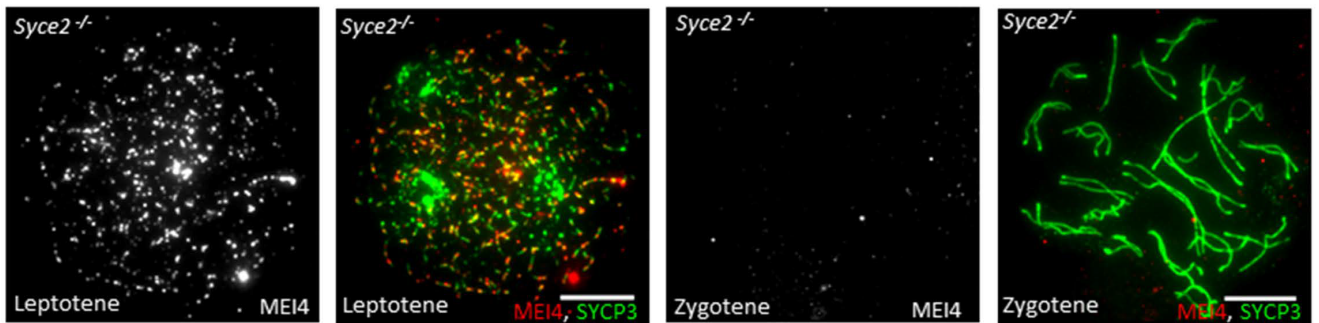


Fig. S4

